This is a preprint, the final version is subject to change, of the American Mineralogist (MSA)
Cite as Authors (Year) Title. American Mineralogist, in press.
(DOI will not work until issue is live.) DOI: http://dx.doi.org/10.2138/am.2014.4450

Revision 1

Enthalpies of Formation of Fe–Ni Monosulfide Solid Solutions

AMIR H. TAVAKOLI and ALEXANDRA NAVROTSKY*

Peter A. Rock Thermochemistry Laboratory and NEAT ORU, University of California, Davis, USA

ABSTRACT

Binary and ternary sulfides in the Fe–Ni–S system are of major fundamental and practical interest in environmental, geological, and planetary science. Despite extensive thermodynamic modeling of phase equilibria, the enthalpies of formation of solid solutions in this system have not been measured directly as functions of both nickel/iron and metal/sulfur ratios. This communication reports enthalpies of formation of Fe-Ni monosulfide solid solutions (*mss* = $(Fe_{1-x}Ni_x)_{1-z}S$, $0 \leq x \leq 1$; $0.875 \leq 1 - z \leq 1$) quenched from 750 ˚C, representing disordered structural states. Measurements were performed on three series of solid solutions using oxidative solution calorimetry in molten sodium molybdate solvent at 702 ˚C. The measured enthalpies of formation of $Ni_{1-z}S$ solid solutions from elements are consistent with prior data reported for a few compositions. The enthalpies of formation of ternary compositions, $(Fe_{1-x}Ni_x)_{1-z}S$, are reported for the first time. Within their uncertainties, the enthalpies of formation of the solid solutions, quenched from high temperature, with respect to the end-members (enthalpies of mixing) at 25 ˚C are zero. An experimentally derived equation is proposed for the calculation of enthalpies of formation of all high temperature monosulfide solid solutions in the Fe–Ni–S system. The thermodynamic stabilization of these disordered solid solutions arises not from energetic terms but from the configurational entropy.

* Corresponding Author, E-mail:anavrotsky@ucdavis.edu

INTRODUCTION

Reflecting their fundamental and practical importance in geological, planetary and environmental science, as well as in technology, binary and ternary compounds in the Fe–Ni–S system have been and continue to be of major interest. Phase equilibria in this system have been widely studied and isothermal sections of the Fe–Ni–S phase diagram have been constructed by both experiments (Kullerud 1963; Craig et al. 1967; Shewman and Clark 1970; Misra and Fleet 1973; Karupmoller and Makovicky 1995; Ebel and Naldrett 1996; Karupmoller and Makovicky 1998; Ueno et al. 2000; Kosyakov et al. 2003; Sack and Ebel 2006) and modeling (Hsieh et al. 1987b; Hsieh et al. 1987c; Kongoli and Pelton 1999; Waldner and Pelton 2004a). These data clearly show the extent and complexity of solid solutions in the ternary Fe–Ni–S system. Fe-Ni monosulfide solid solutions (*mss*), stable over the temperature range 300-1000 °C, form the largest solid solution region in the system, which is continuous from $Fe_{1-z}S$ to $Ni_{1-z}S$ and extends over a range of S contents from 50 to ~ 54 at.% (Naldrett et al. 1967; Vaughan and Craig 1974). Upon slow cooling below 600 °C, the exsolution of low-temperature pentlandite ($(Ni,Fe)_9S_8$) from the *mss* occurs (Durazzo and Taylor 1982; Etschmann et al. 2004). Eventually, the *mss* region becomes discontinuous below 300 °C and instead, two *mss* regions form, one of which extends from $Fe_{1-x}S$ to ~ 25 at.% $Ni_{1-z}S$ and the other extends from $Ni_{1-z}S$ to ~ 30 at.% $Fe_{1-z}S$ (Craig 1973; Misra and Fleet 1973a).

Thermodynamic properties of $Fe_{1-z}S$ solid solutions, as shown in the literature, have been studied comprehensively (Rau 1976; Cemic and Kleppa 1988; Grønvold and Stølen 1995; Robie and Hemingway 1995; Waldner and Pelton 2005; Xu and Navrotsky 2010). Despite many reports on thermodynamic properties of binary $Ni_{1-z}S$ solid solutions (Ariya et al. 1971; Rau 1975; Lin et al. 1978; Cemic and Kleppa 1986; Grønvold and Stølen 1995; Waldner and Pelton

2004b; Arita 2006), more experimentally measured thermochemical data, particularly for the cation deficient compositions, are desirable. The available experimental thermodynamic data for the ternary $(Fe,Ni)_{1-z}S$ hexagonal solid solutions (*mss)* are limited to a few studies addressing sulfur potentials at 700–900 °C (Hsieh et al. 1987a; Kosyakov et al. 2003; Sinyakova and Kosyakov 2006) and heat capacities at 315–444 °C (Drebushchak and Sinyakova 2007). In terms of thermodynamic modeling, the first statistical thermodynamic model was formulated in 1987 (Hsieh et al. 1987b). In 2004, a thermodynamic model was formulated based on the compound-energy formalism using $Fe_{1-x}S$ and $Ni_{1-x}S$ binary-model parameters and considering randomly distributed metal atoms and vacancies for modeling (Waldner and Pelton 2004a). Using such computed thermodynamic data for the ternary $(Fe,Ni)_{1-z}S$ system, separation of energetic and entropic factors may be somewhat uncertain and model dependent. Thus, direct determination of the enthalpies of formation of $(Fe,Ni)_{1-z}S$ *mss* is needed for tracking the change in the thermodynamic properties of the *mss* compositions as functions of both the Ni/(Ni + Fe) molar ratio and cation content across the stability region.

In this work, high temperature oxidative solution calorimetry is applied to determine the enthalpies of formation of $(Fe_{1-x}Ni_x)_{1-z}S$ compositions quenched from 750 ^{o}C with Ni/(Ni + Fe) molar ratios from 0 to 1 ($0 \leq x \leq 1$) and cation contents, ranging from 47.4 to 49.5 at.% ($0.919 \leq 1\text{-}z \leq 0.982$). The measured calorimetric data are analyzed and discussed for three groups of *mss* solid solutions: (a) ternary compositions with various Ni/(Ni + Fe) molar ratios ranging from 0 to 1; (b) ternary compositions with varying cation contents and constant Ni/(Ni + Fe) molar ratios; and (c) binary $Ni_{1-x}S$ compositions. The calorimetric data are then used to derive an equation for the enthalpies of formation of all $(Fe_{1-x}Ni_x)_{1-z}S$ *mss* compositions.

The nature of the calorimetric studies, as shown below, dictates that although the enthalpies of formation refer to room temperature, they represent samples with structural states quenched from the high temperature of synthesis, i.e. to largely disordered *mss* materials.

EXPERIMENTAL METHODS

Synthesis

Fe (< 10 μm powders, 99.9+%, Alfa Aesar), Ni (< 10 μm powders, 99.9+%, Alfa Aesar) and S (powders, 99.9+%, EMD Chemical Inc.) were used as the starting materials. The powder mixtures with Ni/(Ni + Fe) molar ratio from 0 to 1 and sulfur contents from 50.0 to 52.6 at. %, were prepared and then pelletized in a glove box filled with N_2. Each pellet was transferred into an alumina cast ceramic crucible with a lid and then placed in a silica tube and vacuum-sealed. The tubes were first heated in a furnace at 200 °C for 24 hours to transform the starting powder mixtures into sulfides, in order to minimize sulfur loss at elevated temperatures. Next, the tubes were heated at 2 °C/min to 750 °C. After holding at 750 °C for 36 h, the tubes were quenched in cold water to maintain the homogeneous high temperature structure at room temperature.

Characterization

Prior to calorimetry, structural and chemical analyses were required. To check the phase purity of the samples, X-ray diffraction (XRD) patterns were collected using a Bruker AXS D8 Advance diffractometer applying Cu Kα radiation (40 kV/40 mA). Chemical analysis of the samples was carried out using a Cameca SX 100 microprobe operating at 15 kV with 10 nA probe current. Fe $K\alpha_1$, Ni $K\alpha_1$ and S $K\alpha_1$ lines were used for the analysis using LLIF and LPET analytical crystals. Pyrrhotite ($Fe_{0.467}S_{0.533}$), millerite (NiS) and pentlandite ($Fe_{0.265}Ni_{0.265}S_{0.470}$) were used as standards. Secondary electron images were taken to check for surface roughness

and to estimate the average crystallite size. Backscattered electron images and element maps generated by energy-dispersive X-ray spectroscopy were taken to check the homogeneity of the samples.

Calorimetry

High temperature oxidative solution calorimetry was used to determine the enthalpies of formation of the sulfide samples. This method is well developed (Navrotsky 1977; McHale et al. 1996; Navrotsky 1997; Navrotsky 2001) and has been applied previously to study nitrides (Elder et al. 1993; Ranade et al. 2000; Ranade et al. 2001), sulfides (Deore and Navrotsky 2006; Xu and Navrotsky 2010) and selenides (Deore et al. 2008; Xu et al. 2011). Using this technique, ~ 2 mg pellets, made by pressing the powders into a 1mm die, were dropped from room temperature into molten sodium molybdate ($3Na_2O.4MoO_3$) solvent at 702 °C in a custom made Tian-Calvet twin microcalorimeter (Navrotsky 1977; Navrotsky 1997) under oxidizing atmosphere. As the sample dissolves, the sulfide is oxidized to dissolved sulfate in the melt (Deore and Navrotsky 2006; Xu and Navrotsky 2010), the ferrous iron is oxidized to dissolved ferric iron in the melt (Xu and Navrotsky 2010; Lilova et al. 2012), and the nickel dissolves as Ni^{2+} (Wang and Navrotsky 2004). The reaction rate of the pellet with solvent was accelerated and oxidizing conditions maintained by bubbling and flushing oxygen through the solvent at 12 and 60 mL/min, respectively. Six to eight pellets of each composition were dropped to obtain appropriate statistics. The calorimeter was calibrated using the heat content of platinum rods, as described earlier (Liang et al. 1999a; Liang et al. 1999b; Zhang et al. 2006). Although, a ~5 mg pellet is usually dropped for a typical oxide melt solution calorimetric measurement, in this case the relatively slow dissolution rate and the strong exothermic oxidation enthalpy of the sulfide samples made it advantageous to drop a smaller mass of sample, ~ 2 mg. This kept the total

115 reaction time (including the oxidative dissolution and the return of the calorimetric signal to
116 baseline) to within an hour, which helped in the collection of more accurate calorimetric data.
117 Indeed, the high sensitivity and stable baseline signal of the calorimeter enabled the authors to
118 even drop a 0.5 mg pellet. This applies to cases like this work, in which a large heat effect is
119 generated by oxidation reactions.
120

121 ## RESULTS

122 The phase purity of the synthesized compositions, identified as S01-S10, was confirmed
123 by the analysis of the XRD patterns. The average crystallite size was roughly estimated to be 10
124 ± 5 microns using the secondary electron images. No chemical heterogeneity was detected by
125 backscattered electron images and elemental mapping. Therefore, the main source of the
126 uncertainties given in Table I for the chemical compositions, obtained by the electron
127 microprobe analysis, was likely the surface roughness of the pellets.

128 As expected for the high temperature pyrrhotite solid solutions, the crystal structure of
129 the obtained materials is the simple hexagonal NiAs-type. The lattice constants, calculated by
130 cell refinement using Jade 6.1 software, are listed in Table I. In agreement with the literature
131 (Misra and Fleet 1973b), while the "*a*" lattice parameter appears to be insensitive to the
132 metal/sulfur and cation ratios, the "*c*" parameter significantly decreases with increasing Ni/(Ni +
133 Fe) molar ratio.

134 To analyze the calorimetric data, the measured compositions were divided into three
135 groups within the stability limit of monosulfide solid solutions. As can be seen in Figure 1, these
136 groups are: group (a), including six compositions with changing Ni/(Ni + Fe) molar ratios and a
137 slight linear change in sulfur content; group (b), containing three compositions with constant

Ni/(Ni + Fe) molar ratios of 0.6 and varying sulfur content; and group (c), comprising three cation deficient compositions of binary $Ni_{1-z}S$ solid solution.

The oxidative drop solution enthalpies, ΔH_{ds}, are given in Table II. The enthalpies of formation of the *mss* compositions from the constituent elements, ΔH_f, (see Table II) were determined through the thermodynamic cycle given in Table. III. The enthalpies of formation of the *mss* compositions with respect to the *mss* end-members (enthalpies of mixing, ΔH_{mix}) were determined using the thermodynamic cycle in Table IV and listed in Table II. In Figures (2a) and (2b), the enthalpy data (ΔH_{ds} and ΔH_f) obtained for the compositions in group (a) are plotted as a function of the Ni/(Ni + Fe) molar ratio, indicating a linear change of the ΔH_{ds} and ΔH_f data toward less exothermic enthalpy of formation with substitution of Ni. As shown in Figure (2c), the enthalpies of formation of the ternary *mss* compositions from the binary end-members, ΔH_{mix}, are zero within the uncertainties. Considering the enthalpy data for the compositions in group (b) with constant Ni/(Ni + Fe) ratios of 0.6, the ΔH_{ds} and ΔH_f values become slightly less exothermic with a decrease of the cation content (see Figure 3). The ΔH_{mix} value for composition $(Fe_{0.403}Ni_{0.597})_{0.918}S$ in group (b) was 0.1 ± 2.8 kJ/mol (see Table II). In group (c), the binary $Ni_{1-z}S$ compositions, the trend of enthalpy change with cation content appears to be similar to that in group (b). In this connection, as shown in Figure 4, the enthalpies of formation of the $Ni_{1-z}S$ samples increases by ~3 kJ/mol with decrease of ~1.5 mol % Ni. Moreover, the enthalpy of formation of $Ni_{0.953}S$ from the extremes of the solid solution range ($Ni_{0.924}S$ and $Ni_{0.982}S$), ΔH_{mix}, equals 0.7 ± 3.7 kJ/mol, again suggesting a close to zero heat of mixing.

Discussion

To the best of the authors' knowledge, there are no data in the literature for the enthalpies of formation of ternary Fe-Ni *mss* compositions. For high-temperature $Ni_{1-z}S$ pyrrhotite (α-$Ni_{1-z}S$), the enthalpies of formation reported in previous works are plotted in Figure 4 together with the data obtained in this research. The literature data, except the values reported in Ariya et al. (1971), are limited to stoichiometric α-NiS. However, the enthalpy data presented in this report cover a range of cation deficient compositions. The linear fit to our ΔH_f data in Figure 4 can be expressed as: ΔH_f (α-$Ni_{1-z}S$) = [a.(1-z) + b] ± e kJ/mol, where 1-z is the nickel content on the basis of one sulfur, a = –50.0 ± 14.9 kJ/mol; b = –38.8 ± 14.2 kJ/mol; e = 1.9 kJ/mol and R^2 = 0.92. By extrapolation of the fitted line to 1-z = 1, it was determined that ΔH_f (α-NiS) = –88.8 ± 1.9 kJ/mol. This is in good agreement with the reported data: –84.9 ± 2.5 kJ/mol (Ariya et al. 1971), –88.1 ± 1.0 kJ/mol (Cemic and Kleppa 1986), and –87.0 kJ/mol (Waldner and Pelton 2004b). In terms of the ΔH_f values obtained for the nonstoichiometric compositions, while the results reported here show a trend toward more exothermic enthalpies of formation for the compositions with less cation deficiency, the trend of the enthalpy change given in Ariya et al. (1971) is the opposite (see Figure 4). The trend shown by the authors' results appears reasonable since the enthalpy of formation of a cation vacancy in a crystalline structure is always considered to be endothermic, which means that the enthalpies of formation of the cation deficient compositions (α-$Ni_{1-z}S$) are expected to be less exothermic than that of stoichiometric NiS. Consistent with these results, the enthalpies of formation of the cation deficient $Fe_{1-z}S$ compositions have been reported to be less exothermic than that of stoichiometric FeS (Grønvold and Stølen 1992; Waldner and Pelton 2005; Xu and Navrotsky 2010).

The enthalpies of formation of the binary and ternary solid solutions with respect to the end-members, ΔH_{mix}, for all the compositions investigated in this work were shown to be zero

within the error limits, similar to the calorimetric results reported before for the $Fe_{1-z}S$ solid solutions (Xu and Navrotsky 2010). On the microscopic scale, such zero heats of mixing suggest the absence of significant strain energy. This would lead to positive heats of mixing, or of ordering of cations and vacancies at intermediate compositons, which would lead to negative enthalpies of mixing. These observations are consistent with the preservation of a largely disordered structural state upon quenching the samples to room temperature.

Although a zero heat of mixing is often interpreted to imply "ideal" mixing behavior, strictly speaking an ideal solution in a binary system A–B is one in which the entropy of mixing, per mole of solution, is given by an expression consistent with Raoult's Law (activity of a component equal to its mole fraction)

$$\Delta S_{mix} = -R\,[X\ln X + (1-X)\ln(1-X)] \qquad (1)$$

where X is the mole fraction of one of the components. Statistically, this implies that there is random mixing of two (and only two) species on one mole of sites in the system, and that the end-members themselves have no configurational entropy. This is not the case in the Fe-Ni-S system because of the variability of the Ni/(Ni + Fe) and metal/sulfur ratios and the existence of cation vacancies. Thus, despite zero heat of mixing, the *mss* phases are not ideal *sensu stricto* or, in other words, they are non-Raoultian solid solutions. Rather, the entropy of mixing, ΔS_{mix}, for $(Fe_{1-x}Ni_x)_{1-z}S$ solid solutions can be calculated by assuming that cation vacancies and cationic species are randomly distributed, ignoring any possible interactions between the defects. Accordingly, ΔS_{mix} equals the total configurational entropy, S_{conf}, of $(Fe_{1-x}Ni_x)_{1-z}S$ solid solutions

minus that of a weighted average of the respective end-members in Eqs. (1), (5) and (9), as listed in Table IV, where S_{conf} is

$$S_{conf} = -R[(1-z)x\ln(x) + (1-z)(1-x)\ln(1-x) + (1-z)\ln(1-z) + z\ln(z)]; \ (0 \le x \le 1;\ 0.018 \le z \le 0.101). \quad (2)$$

with 1-z and x defined as above. In this equation, the first two terms arise from the random mixing of Fe and Ni cations while the last two terms arise from the cation-vacancy mixing in the system. The values of S_{conf}, ΔS_{mix}, and $\Delta G_{mix\text{-}calc}$ calculated for the $(Fe_{1-x}Ni_x)_{1-z}S$ solid solutions are given in Table V. In addition, the $\Delta G_{mix\text{-}calc}$ data determined for the ternary *mss* with respect to the binary end-members are plotted as a function of Ni/(Ni + Fe) ratio in Figure 5(a). These data indicate more negative Gibbs free energies of mixing compared to cases with simple ideal one-site mixing, like $Ni_{1-z}S$ solid solutions, because of both Fe - Ni mixing and cation deficiency. The ΔG_{mix} values, based on the change in configurational entropy ($\Delta G_{mix\text{-}calc} = -T\Delta S_{mix}$), were calculated for the two series of solid solutions, for which the experimental data obtained from measuring S_2 fugacity (f_{S2}) have been reported. Figure 5(b) shows the Gibbs free energies of mixing of the $(Fe_{0.454}Ni_{0.546})_{1-z}S$ solid solutions from S_2-fugacity measurements ($\Delta G_{mix\text{-}exp}$) at 699 ˚C (Hsieh et al. 1987a) and from the authors' calculations ($\Delta G_{mix\text{-}calc}$). Similarly, in Figure 5(c), the Gibbs free energies of mixing of $Ni_{1-z}S$ solid solutions from S_2 fugacity measurements ($\Delta G_{mix\text{-}exp}$) at 713 ˚C (Rau 1975) and from the authors' calculations ($\Delta G_{mix\text{-}calc}$) are plotted. As indicated in Figures 5(b) and 5(c), the Gibbs free energies of mixing obtained from both sulfur fugacity measurements and thermochemical calculations match with a difference less than 0.03 kJ/mol. Similarly, overlapping values of ΔG_{mix} calculated from thermochemical data and ΔG_{mix} measured from sulfur fugacity data for the $Fe_{1-z}S$ solid solution have been reported (Xu and

Navrotsky 2010). We conclude that for Fe-Ni-S *mss* samples with a structural state quenched from high temperature, the enthalpies of mixing are zero and the Gibbs energies of mixing are well represented by the change in configuratonal entropy for a maximally disordered solid solution. This work does not address the appearance of more ordered states at lower temperatures. The exsolution of pentlandite $(Ni,Fe)_9S_8$ from the Fe-Ni *mss* upon slow cooling is believed to be a result of vacancy ordering, as also suggested by Etschmann et al. (2004), and not due to positive enthalpy of mixing.

Zero enthalpies of mixing, as found in this work, signify that the enthalpies of formation of Fe-Ni solid solutions from elements (ΔH_f) should change linearly as a function of the Ni/(Ni + Fe) molar ratio at a constant cation content as well as being a linear function of the cation content at a fixed Ni/(Ni + Fe) molar ratio, as can be seen in Figures 2 to 4. Therefore, the enthalpy of formation of a Fe-Ni *mss* with the empirical formula of $(Fe_{1-x}Ni_x)_{1-z}S$ can be determined using the following equation:

$$\Delta H_f\,(Fe_{1-x}Ni_x)_{1-z}S = c.(1-z) + d.x + e, \quad (T = 25\ ^\circ C;\ 0.875 \le 1-z \le 1;\ 0 \le x \le 1;) \tag{3}$$

where

$$c = \left(\frac{\partial \Delta H_f}{\partial (1-z)}\right)_x, \tag{4}$$

$$d = \left(\frac{\partial \Delta H_f}{\partial x}\right)_{1-z}, \tag{5}$$

and e is a constant. The enthalpies of formation of the three series of solid solutions obtained for groups (a), (b), and (c) in this work plus the enthalpies of formation of the $Fe_{1-z}S$ *mss*, previously published by Xu and Navrotsky (2010), were used to model the relationship between the enthalpy of formation and the two variables, 1-z and x, in Equation 3. The best fit to the data by least squares multiple linear regression yields Equation 6:

$$\Delta H_f\,(Fe_{1-x}Ni_x)_{1-z}S = [-55.1(1-z) + 12.6x - 46.2] \pm 1.8\ \text{kJ/mol};\ R^2 = 0.98\ \ (T = 25\ ^\circ\text{C};\ 0.875 \le 1\text{-}z \le 1;\ 0 \le x \le 1;). \quad (6)$$

To check the precision of Equation 6 for calculating the enthalpies of formation of monosulfide solid solutions over the broad stability region in the Fe–Ni–S system, we calculated ΔH_f for the *mss* compositions studied both in this work and in Xu and Navrotsky (2010). The calculated enthalpies along with the enthalpies determined based on the calorimetric measurements, as listed in Table VI, indicate a very good match within experimental uncertainties. Equation 6 for enthalpy of formation together with Equation 2 for configurational entropy can be used to calculate Gibbs free energy of formation ($\Delta G_f = \Delta H_f - T\Delta S_{conf}$) and activities of components in the high temperature range where ordering is minor, namely above about 500 ^oC. This simple model can be used as a first approxination in calculating Fe–Ni–S equilibria and the reactions of these sulfides with other phases at temperatures between about 500 ^oC and the onset of melting.

ACKNOWLEDGMENTS

This research received support from the U.S. Department of Energy, Grant DE-FG02-97ER14749. We thank Nick W. Botto for his assistance in the chemical analysis.

272

273 # REFERENCES

274 Arita, M. (2006) Thermodynamics of the solid Ni-S system. Metallurgical and Materials
275 Transactions A-Physical Metallurgy and Materials Science, 37A, 3009-3022.
276 Ariya, S.M., Morozova, M.P., Pavlinova, L.A., and Ponomareva, V.L. (1971) Entalpies of
277 formation of nickel sulfides. Zhurnal Fizicheskoi Khimii, 45, 2385-6.
278 Cemic, L., and Kleppa, O.J. (1986) High-temperature calorimetry of sulfide systems .1.
279 Thermochemistry of liquid and solid-phases of Ni + S. Geochimica Et Cosmochimica
280 Acta, 50, 1633-1641.
281 ---------(1988) High-temperature calorimetry of sulfide systems .3. Standard enthalpies of
282 formation of phases in the systems Fe-Cu-S and Co-S. Physics and Chemistry of
283 Minerals, 16, 172-179.
284 Craig, J.R. (1973) Pyrite-pentalandite assemblages and other low-temperature relations in Fe-Ni-
285 S system. American Journal of Science, A273, 496-510.
286 Craig, J.R., Naldrett, A.J., and Kullerud, G. (1967) The Fe-Ni-S sustem: 400 ^{o}C isothermal
287 diagram. . Carnegie Inst. Washington Yearbook, 66, p. 440-441.
288 Deore, S., and Navrotsky, A. (2006) Oxide melt solution calorimetry of sulfides: Enthalpy of
289 formation of sphalerite, galena, greenockite, and hawleyite. American Mineralogist, 91,
290 400-403.
291 Deore, S., Xu, F., and Navrotsky, A. (2008) Oxide-melt solution calorimetry of selenides:
292 Enthalpy of formation of zinc, cadmium, and lead selenide. American Mineralogist, 93,
293 779-783.

Drebushchak, V.A., and Sinyakova, E.F. (2007) Calorimetric search for the discontinuity in $Fe_{0.96}S$-$Ni_{0.96}S$ solid solutions. Journal of Thermal Analysis and Calorimetry, 89, 303-307.

Durazzo, A., and Taylor, L.A. (1982) Exsolution in the mss-pentlandite system - textural and genetic-implications for Ni-sulfide ores. Mineralium Deposita, 17, 313-332.

Ebel, D.S., and Naldrett, A.J. (1996) Fractional crystallization of sulfide ore liquids at high temperature. Economic Geology and the Bulletin of the Society of Economic Geologists, 91, 607-621.

Elder, S.H., Disalvo, F.J., Topor, L., and Navrotsky, A. (1993) Thermodynamics of ternary nitride formation by ammonolysis - application to $LiMON_2$, Na_3WN_3, and Na_3WO_3N. Chemistry of Materials, 5, 1545-1553.

Etschmann, B., Pring, A., Putnis, A., Grguric, B.A., and Studer, A. (2004) A kinetic study of the exsolution of pentlandite $(Ni,Fe)_9S_8$ from the monosulfide solid solution (Fe,Ni)S. American Mineralogist, 89, 39-50.

Grønvold, F., and Stølen, S. (1992) Thermodynamics of iron sulfides .2. Heat-capacity and thermodynamic properties of FeS and of $Fe_{0.875}S$ at temperatures from 298.15 to 1000 K, of $Fe_{0.98}S$ from 298.15 to 800 K, and of $Fe_{0.89}S$ from 298.15 to about 650 K - thermodynamics of formation. Journal of Chemical Thermodynamics, 24, 913-936.

-------- (1995) Heat capacity and thermodynamic properties of millerite from 298.15 to 660 K and NiAs-type nickel(ii) sulfide from 260 to 1000 K. Thermodynamics of the NiAs-type to millerite transition. Thermochimica Acta, 266, 213-229.

Hsieh, K.C., Kao, M.Y., and Chang, Y.A. (1987a) A thermogravimetric investigation of the Fe-Ni-S system from 700 to 900 ^{o}C. Oxidation of Metals, 27, 123-141.

Hsieh, K.C., Schmid, R., and Chang, Y.A. (1987b) The Fe-Ni-S system .2. A thermodynamic model for the ternary monosulfide phase with the nickel arsenide structure. High Temperature Science, 23, 39-52.

Hsieh, K.C., Vlach, K.C., and Chang, Y.A. (1987c) The Fe-Ni-s system .1. A thermodynamic analysis of the phase-equilibria and calculation of the phase-diagram from 1173 K to 1623 K. High Temperature Science, 23, 17-38.

Karupmoller, S., and Makovicky, E. (1995) The phase system Fe-Ni-S at 725 ^{o}C. Neues Jahrbuch Fur Mineralogie-Monatshefte1-10.

-------- (1998) The phase system Fe-Ni-S at 900 ^{o}C. Neues Jahrbuch Fur Mineralogie-Monatshefte373-384.

Kongoli, F., and Pelton, A.D. (1999) Model prediction of thermodynamic properties of Co-Fe-Ni-S mattes. Metallurgical and Materials Transactions B-Process Metallurgy and Materials Processing Science, 30, 443-450.

Kosyakov, V.I., Sinyakova, E.F., and Shestakov, V.A. (2003) Dependence of sulfur fugacity on the composition of phase associations in the Fe-FeS-NiS-Ni system at 873 K. Geochemistry International, 41, 660-669.

Kullerud, G. (1963) The Fe-Ni-S system. Carnegie Inst. Washington Yearbook, 62, p. 175-189.

Liang, J.J., Navrotsky, A., Leppert, V.J., Paskowitz, M.J., Risbud, S.H., Ludwig, T., Seifert, H.J., Aldinger, F., and Mitomo, M. (1999a) Thermochemistry of $Si_{6-z}Al_zO_zN_{8-z}$ (z=0 to 3.6) materials. Journal of Materials Research, 14, 4630-4636.

Liang, J.J., Topor, L., Navrotsky, A., and Mitomo, M. (1999b) Silicon nitride: Enthalpy of formation of the alpha- and beta-polymorphs and the effect of C and O impurities. Journal of Materials Research, 14, 1959-1968.

Lilova, K.I., Xu, F., Rosso, K.M., Pearce, C.I., Kamali, S., and Navrotsky, A. (2012) Oxide melt solution calorimetry of Fe-bearing oxides and application to the magnetite-maghemite (Fe_3O_4-$Fe_{8/3}O_4$) system. American Mineralogist, 97, 164-175.

Lin, R.Y., Hu, D.C., and Chang, Y.A. (1978) Thermodynamics and phase relationships of transition metal-sulfur systems .2. Nickel-Sulfur system. Metallurgical Transactions B-Process Metallurgy, 9, 531-538.

McHale, J.M., Kowach, G.R., Navrotsky, A., and DiSalvo, F.J. (1996) Thermochemistry of metal nitrides in the Ca/Zn/N system. Chemistry-A European Journal, 2, 1514-1517.

Misra, K.C., and Fleet, M.E. (1973a) Chemical compositions of synthetic and natural pentlandite assemblages. Economic Geology, 68, 518-539.

---------(1973b) Unit cell parameters of monosulfide, pentlandite, and taenataite solid soultions within the Fe-Ni-S system. Materials Science Bulletin, 8, 669-678.

Naldrett, A.J., Craig, J.R., and Kullerud, G. (1967) The central portion of the Fe-Ni-S system and its bearing on pentlandite exclusion in iron-nickel sulfide ores Economic Geology, 62, 826-847.

Navrotsky, A. (1977) Progress and new directions in high-temperature calorimetry. Physics and Chemistry of Minerals, 2, 89-104.

Navrotsky, A. (1997) Progress and new directions in high temperature calorimetry revisited. Physics and Chemistry of Minerals, 24, 222-241.

Navrotsky, A. (2001) Thermochemical studies of nitrides and oxynitrides by oxidative oxide melt calorimetry. Journal of Alloys and Compounds, 321, 300-306.

Ranade, M.R., Tessier, F., Navrotsky, A., Leppert, V.J., Risbud, S.H., DiSalvo, F.J., and Balkas, C.M. (2000) Enthalpy of formation of gallium nitride. Journal of Physical Chemistry B, 104, 4060-4063.

Ranade, M.R., Tessier, F., Navrotsky, A., and Marchand, R. (2001) Calorimetric determination of the enthalpy of formation of inn and comparison with aln and gan. Journal of Materials Research, 16, 2824-2831.

Rau, H. (1975) Range of homogeneity and defect interaction in high-temperature nickel sulfide $Ni_{1-x}S$. Journal of Physics and Chemistry of Solids, 36, 1199-1204.

------- (1976) Energetics of defect formation and interaction in pyrrhotite $Fe_{1-x}S$ and its homogeneity range. Journal of Physics and Chemistry of Solids, 37, 425-429.

Robie, R.A., and Hemingway, B.S. (1995) Thermodynamic properties of minerals and related substances at 298.15 K and 1 bar (105 pascals) presuure and at higher temperatures. U.S. Geological Survey Bulletin, Washington.

Sack, R.O., and Ebel, D.S. (2006) Thermochemistry of sulfide mineral solutions. In D.J. Vaughan, Ed. Sulfide mineralolgy and geochemistry, 61, p. 265-364.

Shewman, R.W., and Clark, L.A. (1970) Pentlandite phase relations in the Fe-Ni-S system and notes on the monosulfide solid solutions. Canadian Journal of Earth Science, 7, 67-85.

Sinyakova, E.F., and Kosyakov, V.I. (2006) Phase relationships and sulfur fugacity in the system Fe-FeS-NiS-Ni at 900^{o}C. Russian Geology and Geophysics, 47, 835-846.

Ueno, T., Ito, S., and Nakatsuka, S. (2000) Phase equilibria in the system Fe-Ni-S at 500 ^{o}C and 400 ^{o}C. Journal of Mineralogical and Petrological Sciences, 95, 145-161.

Vaughan, D.J., and Craig, J.R. (1974) Crystal-chemistry and magnetic-properties of iron in monosulfide solid-solution of Fe-Ni-S system. American Mineralogist, 59, 926-933.

Waldner, P., and Pelton, A.D. (2004a) Critical thermodynamic assessment and modeling of the Fe-Ni-S system. Metallurgical and Materials Transactions B-Process Metallurgy and Materials Processing Science, 35, 897-907.

Waldner, P., and Pelton, A.D. (2004b) Thermodynamic modeling of the Ni-S system. Zeitschrift Fur Metallkunde, 95, 672-681.

Waldner, P., and Pelton, A.D. (2005) Thermodynamic modeling of the Fe-S system. Journal of Phase Equilibria and Diffusion, 26, 23-38.

Wang, M.J., Navrotsky, A., (2004) Enthalpy of formation of $LiNiO_2$, $LiCoO_2$ and their solid solution, $LiNi_{1-x}Co_xO_2$. Solid State Ionics, 166, 167-173.

Xu, F., and Navrotsky, A. (2010) Enthalpies of formation of pyrrhotite $Fe_{1-0.125x}S$ ($0 \leq x \leq 1$) solid solutions. American Mineralogist, 95, 717-723.

Xu, F., Zhou, W., and Navrotsky, A. (2011) Cadmium selenide: Surface and nanoparticle energetics. Journal of Materials Research, 26, 720-725.

Zhang, Y.H., Navrotsky, A., and Sekine, T. (2006) Energetics of cubic Si_3N_4. Journal of Materials Research, 21, 41-44.

411 **FIGURE CAPTIONS**

412 Figure 1. Compositions of $(Fe_{1-x}Ni_x)_{1-z}S$ solid solutions, denoted by filled circles, divided into
413 three groups of (a), (b), and (c) in order to investigate the effects of Ni/(Ni + Fe) ratio and cation
414 content, separately, on the enthalpies of formation of the solid solutions. Grey area in this figure
415 represents the stability region of Fe-Ni monosulfide solid solutions at 750 ˚C according to our
416 synthesis results. Upper and lower limits of this region can hardly be determined by experiments
417 and may not be precise.

418
419 Figure 2. (a) enthalpies of oxidative drop solution in sodium molybdate melt at 702 ˚C, ΔH_{ds}, (b)
420 enthalpies of formation from elements at 25 ˚C, ΔH_f, and (c) enthalpies of formation from the
421 binary end-members (enthalpies of mixing) at 25 ˚C, ΔH_{mix}, plotted as a function of the Ni/(Ni +
422 Fe) molar ratio for the ternary monosulfide solid solutions in group (a), which are extended from
423 the Fe-rich side to Ni-rich side in the Fe–Ni–S system.

424

425 Figure 3. Enthalpies of oxidative drop-solution at 702 ˚C, ΔH_{ds}, (filled circles) and enthalpies of
426 formation from elements at 25 ˚C, ΔH_f (open circles) plotted as a function of the cation content
427 for the $(Fe_{0.40}Ni_{0.60})_{1-z}S$ solid solutions in group (b).

428

429 Figure 4. Enthalpies of formation of $Ni_{1-z}S$ solid solutions from elements at 25 ˚C, ΔH_f, plotted
430 as a function of the nickel content. The data obtained in this work for the compositions in group
431 (c) are denoted by filled circles and those reported in the literature are denoted by open symbols.

432

433 Figure 5. Gibbs free energies of mixing, $\Delta G_{mix\text{-}calc}$, of (a) $(Fe_{1-x}Ni_x)_{1-z}S$ compositions extended
434 from $Fe_{0.919}S$ to $Ni_{0.953}S$ at 700 °C, (b) $(Fe_{0.454}Ni_{i0.545})_{1-z}S$ compositions at 699 ˚C, and (c) $Ni_{1-z}S$

compositions at 713 ˚C. Solid curves represent the calculated values from $-T\Delta S_{mix}$, $\Delta G_{mix\text{-}calc}$. Filled circles in (b) and (c) are calculated values from measuring S_2 fugacity, $\Delta G_{mix\text{-}exp}$, reported in (Hsieh et al. 1987a) and (Rau 1975), respectively.

438

439 Table I. Chemical compositions, empirical formula and lattice parameters of the synthesized $(Fe_{1-x}Ni_x)_{1-z}S$ solid solutions.
440

Sample ID	Chemical composition			Empirical formula	Lattice parameters[#]	
	Fe	Ni	S	$(Fe_{1-x}Ni_x)_{1-z}S$, $(0 \le x \le 1; 0.018 \le z \le 0.101)$	a (nm)	c (nm)
S01	61.6 ± 0.1 (47.9)[*]	---	38.5 ± 0.1 (52.1)	$Fe_{0.919}S$	3.4491 (5)[†]	5.7519 (7)
S02	49.2 ± 0.2 (38.6)	12.7± 0.1 (9.5)	38.0 ± 0.2 (51.9)	$(Fe_{0.802}Ni_{0.198})_{0.927}S$	3.4440 (6)	5.6839 (6)
S03	36.6 ± 0.4 (29.0)	25.7 ± 0.5 (19.3)	37.5± 0.1 (51.7)	$(Fe_{0.601}Ni_{0.399})_{0.934}S$	3.4386 (3)	5.6194 (4)
S04	24.0 ± 0.3 (19.0)	37.8 ± 0.3 (28.4)	38.3 ± 0.1 (52.6)	$(Fe_{0.401}Ni_{0.599})_{0.899}S$	3.4217 (6)	5.4106 (7)
S05	24.4 ± 0.2 (19.3)	37.9 ± 0.3 (28.6)	37.8 ± 0.1 (52.1)	$(Fe_{0.403}Ni_{0.597})_{0.918}S$	3.4283 (4)	5.4621 (9)
S06	24.7 ± 0.2 (19.6)	38.2 ± 0.2 (28.7)	37.6 ± 0.5 (51.7)	$(Fe_{0.406}Ni_{0.594})_{0.934}S$	3.4359 (6)	5.5290 (6)
S07	12.2 ± 0.1 (9.8)	50.3 ± 0.1 (38.6)	36.8 ± 0.4 (51.6)	$(Fe_{0.202}Ni_{0.798})_{0.938}S$	3.4282 (6)	5.3785 (12)
S08	---	63.0 ± 0.2 (48.0)	37.2 ± 0.1 (52.0)	$Ni_{0.924}S$	3.4275 (5)	5.3202 (6)
S09	---	63.4 ± 0.3 (48.8)	36.2 ± 0.3 (51.2)	$Ni_{0.953}S$	3.4334 (1)	5.3326 (1)
S10	---	64.5 ± 0.2 (49.5)	35.8 ± 0.1 (50.5)	$Ni_{0.982}S$	3.4393 (4)	5.3494 (5)

[*] wt.%, at.% in parentheses.

[#] NiAs type structure (Hexagonal, $P6_3/mmc$).

[†] The numbers in parentheses are uncertainties in last digit(s) estimated from least square analysis.

441 Table II. Enthalpies of oxidative drop-solution at 702 ˚C, ΔH_{ds}, enthalpies of formation from the elements, ΔH_f, and enthalpies of

442 formation from the end-members, ΔH_{mix}, for the three groups of $(Fe_{1-x}Ni_x)_{1-z}S$ solid solutions investigated in this work.

443

Solid solutions group ID	Sample composition	ΔH_{ds} (kJ/mol)	ΔH_f (kJ/mol)	ΔH_{mix} (kJ/mol)[#]
(a)	$Fe_{0.919}S$	−887.0 ± 1.4 (7)[*]	−96.1 ± 2.8	0
	$(Fe_{0.802}Ni_{0.198})_{0.927}S$	−862.2 ± 1.9 (7)	−94.1 ± 3.1	0.6 ± 2.3
	$(Fe_{0.601}Ni_{0.399})_{0.934}S$	−837.1 ± 1.8 (6)	−91.0 ± 2.9	1.7 ± 2.3
	$(Fe_{0.406}Ni_{0.594})_{0.934}S$	−807.9 ± 2.0 (7)	−90.5 ± 3.0	−1.7 ± 2.6
	$(Fe_{0.202}Ni_{0.798})_{0.938}S$	−782.4 ± 2.6 (6)	−86.0 ± 3.5	0.1 ± 3.4
	$Ni_{0.953}S$	−754.8 ± 2.8 (8)	−86.0 ± 3.6	0
(b)	$(Fe_{0.401}Ni_{0.599})_{0.899}S$	−798.4 ± 3.0 (8)	−89.3 ± 3.8	0
	$(Fe_{0.403}Ni_{0.597})_{0.918}S$	−803.7 ± 2.2 (7)	−89.7 ± 3.2	0.1 ± 2.8
	$(Fe_{0.406}Ni_{0.594})_{0.934}S$	−807.9 ± 2.0 (7)	−90.5 ± 3.0	0
(c)	$Ni_{0.924}S$	−749.2 ± 3.4 (6)	−85.3 ± 4.1	0
	$Ni_{0.953}S$	−754.8 ± 2.8 (8)	−86.0 ± 3.6	0.7 ± 3.7
	$Ni_{0.982}S$	−759.0 ± 3.3 (8)	−88.2 ± 4.0	0

*Uncertainties are two standard deviations of the mean. Numbers in parentheses are the number of the experiments.
[#] Data represents the enthalpies of formation from the end-members in each group of the monosulfide solid solutions.

444
445
446

Table III. Thermodynamic cycle for calculating enthalpies of formation of the $(Fe_{1-x}Ni_x)_{1-z}S$ solid solutions from elements at 25 ˚C, ΔH_f.

Reactions	**Enthalpy, ΔH (kJ/mol)**
(1) $(Fe_{1-x}Ni_x)_{1-z}S$ (s, 25 ˚C) + $(1.5+0.75(1-z)-0.25(1-z)x)O_2$ (g, 702 ˚C) = $(1-z)(1-x)\ Fe^{3+}$ (soln, 702 ˚C) + $(1-z)x\ Ni^{2+}$ (soln, 702 ˚C) + SO_4^{2-} (soln, 702 ˚C) + $(1.5(1-z)-0.5(1-z)x-1)O^{2-}$ (soln, 702 ˚C) $(0 \le x \le 1;\ 0.919 \le 1-z \le 0.982)$	$\Delta H_1 = \Delta H_{ds}$ *
(2) Fe_2O_3 (s, 25 ˚C) = $2Fe^{3+}$ (soln, 702 ˚C) + $3O^{2-}$ (soln, 702 ˚C)	$\Delta H_2 = 95.2 \pm 0.8$ #
(3) NiO (s, 25 ˚C) = Ni^{2+} (soln, 702 ˚C) + O^{2-} (soln, 702 ˚C)	$\Delta H_3 = 31.3 \pm 0.6$ †
(4) S (s, 25 ˚C) + $1.5O_2$ (s, 25 ˚C) = SO_3 (s, 25 ˚C)	$\Delta H_4 = -395.7 \pm 0.7$ ‡
(5) SO_3 (s, 25 ˚C) + O^{2-} (soln, 25 ˚C) = SO_4^{-2} (soln, 702 ˚C)	$\Delta H_5 = -203.8 \pm 2.1$ #
(6) 2Fe (s, 25 ˚C) + $1.5O_2$ (g, 25 ˚C) = Fe_2O_3 (s, 25 ˚C)	$\Delta H_6 = -826.2 \pm 1.3$ ‡
(7) Ni (s, 25 ˚C) + $0.5O_2$ (g, 25 ˚C) = NiO (s, 25 ˚C)	$\Delta H_7 = -239.3 \pm 0.4$ ‡
(8) O_2 (g, 25 ˚C) = O_2 (g, 702 ˚C)	$\Delta H_8 = 21.8 \pm 0.0$ ‡
(9) $(1-z)(1-x)$ Fe (s, 25 ˚C) + $(1-z)x$ Ni (s, 25 ˚C) + S (s, 25 ˚C) = $(Fe_{1-x}Ni_x)_{1-z}S$ (s, 25 ˚C) $(0 \le x \le 1;\ 0.919 \le 1-z \le 0.982)$	$\Delta H_9 = \Delta H_f$
$\Delta H_f = -\Delta H_1 + 0.5(1-z)(1-x)\Delta H_2 + (1-z)x\Delta H_3 + \Delta H_4 + \Delta H_5 + 0.5(1-z)(1-x)\Delta H_6 + (1-z)x\Delta H_7 - (1.5+0.75(1-z)-0.25(1-z)x)\Delta H_8$	

* Experimental data from Table II.

Taken from Xu and Navrotsky (2010).

† Drop-solution enthalpy of NiO measured for this work.

‡ Taken from Robie and Hemingway (1995).

Table IV. Thermodynamic cycles for calculating enthalpies of formation of the $(Fe_{1-x}Ni_x)_{1-z}S$ solid solutions from end-members(enthalpies of mixing, ΔH_{mix}) at 25 ˚C.

Reactions	Enthalpy, ΔH (kJ/mol)
(a) $(Fe_{1-x}Ni_x)_{1-z}S$ solid solutions, group (a)	
(1) $(1-x)/(1-0.0357x)\ Fe_{0.919}S + 0.9643x/(1-0.0357x)\ Ni_{0.953}S \approx (Fe_{1-x}Ni_x)_{1-z}S^*$ $(0 \le x \le 1;\ 1-z \approx 0.919/(1-0.0357x))$	$\Delta H_1 = \Delta H_{mix}$
(2) $Fe_{0.919}S$ (s, 25 ˚C) + 2.1892 O_2 (g, 702 ˚C) = 0.919 Fe^{3+} + SO_4^{2-} + 0.3785 O^{2-}	$\Delta H_2 = \Delta H_{ds} = -887.0 \pm 1.3$
(3) $Ni_{0.953}S$ (s, 25 ˚C) +1.9765 O_2 (g, 702 ˚C) + 0.047 O^{2-}(soln, 702 ˚C) = 0.953 Ni^{2+} + SO_4^{2-}	$\Delta H_3 = \Delta H_{ds} = -754.8 \pm 2.8$
(4) $(Fe_{1-x}Ni_x)_{1-z}S$ (s, 25 ˚C) + $(1.5+0.75(1-z)-0.25(1-z)x)O_2$ (g, 702 ˚C) = $(1-z)(1-x)\ Fe^{3+}$ + $(1-z)x\ Ni^{2+}$ + SO_4^{2-} + $(1.5(1-z)-0.5(1-z)x-1)O^{2-}$ $(0 \le x \le 1;\ 1-z \approx 0.919/(1-0.0357x))$	$\Delta H_4 = \Delta H_{ds}^{\#}$
$\Delta H_{mix} \approx (1-x)/(1-0.0357x)\Delta H_1 + 0.9643x/(1-0.0357x)\Delta H_2 - \Delta H_3$	
(b) $(Fe_{0.4}Ni_{0.6})_{1-z}S$ solid solutions, group (b)	
(5) 0.457 $(Fe_{0.401}Ni_{0.599})_{0.899}S$ + 0.543 $(Fe_{0.406}Ni_{0.594})_{0.934}S$ = $(Fe_{0.403}Ni_{0.597})_{0.918}S$	$\Delta H_5 = \Delta H_{mix}$
(6) $(Fe_{0.401}Ni_{0.599})_{0.899}S$ (s, 25 ˚C) + 2.039 O_2 (g, 702 ˚C) = 0.360 Fe^{3+} + 0.538 Ni^{2+} + SO_4^{2-} + 0.078 O^{2-}	$\Delta H_6 = \Delta H_{ds} = -798.4 \pm 3.0$
(7) $(Fe_{0.406}Ni_{0.594})_{0.934}S$ (s, 25 ˚C) + 2.062 O_2 (g, 702 ˚C) = 0.379 Fe^{3+} + 0.555 Ni^{2+} + SO_4^{2-} + 0.124 O^{2-}	$\Delta H_7 = \Delta H_{ds} = -807.9 \pm 2.0$
(8) $(Fe_{0.403}Ni_{0.597})_{0.918}S$ (s, 25 ˚C) + 2.051 O_2 (g, 702 ˚C) = 0.370 Fe^{3+} + 0.548 Ni^{2+} + SO_4^{2-} + 0.103 O^{2-}	$\Delta H_8 = \Delta H_{ds} = -803.7 \pm 2.2$
$\Delta H_{mix} = 0.457\ \Delta H_6 + 0.543\ \Delta H_7 - \Delta H_8 = 0.1 \pm 2.8$ kJ/mol	
(c) $Ni_{1-z}S$ solid solutions, group (c)	
(9) 0.500 $Ni_{0.924}S$ + 0.500 $Ni_{0.982}S$ = $Ni_{0.953}S$	$\Delta H_9 = \Delta H_{mix}$
(10) $Ni_{0.924}S$ (s, 25 ˚C) + 1.924 O_2 (g, 702 ˚C) = 0.924 Ni^{2+} + SO_4^{2-} (soln, 702 C) − 0.152 O^{2-}	$\Delta H_{10} = \Delta H_{ds} = -749.2 \pm 3.4$
(11) $Ni_{0.982}S$ (s, 25 ˚C) + 1.982 O_2 (g, 702 ˚C) = 0.982 Ni^{2+} + SO_4^{2-} (soln, 702 C) − 0.036 O^{2-}	$\Delta H_{11} = \Delta H_{ds} = -759.0 \pm 3.3$
(12) $Ni_{0.953}S$ (s, 25 ˚C) + 1.953 O_2 (g, 702 ˚C) = 0.953 Ni^{2+} + SO_4^{2-} (soln, 702 C) − 0.094 O^{2-}	$\Delta H_{12} = \Delta H_{ds} = -754.8 \pm 2.8$
$\Delta H_{mix} = 0.500\ \Delta H_{10} + 0.500\ \Delta H_{11} - \Delta H_{12} = 0.7 \pm 3.7$ kJ/mol	

* Reaction products are all dissolved in sodium molybdate at 702 ˚C except reactions (1), (5) and (9) in which the reactants and products are solids at 25 C.

Experimental data from Table II.

459
460

461 Table V. Configurational entropies, S_{conf}, entropies of mixing, ΔS_{mix}, and Gibbs free energies of mixing, ΔG_{mix}, of the $(Fe_{1-x}Ni_x)_{1-z}S$

462 compositions calculated at 25°C for the three groups of the solid solutions studied in this work.

463

Solid solutions group ID	**Sample composition**	S_{conf} **(J/mol.K)**	ΔS_{mix} **(J/mol.K)**	$\Delta G_{mix\text{-}cal}$ **(-$T\Delta S_{mix}$) at 700˚C (kJ/mol)**
(a)	$Fe_{0.919}S$	2.34	0	0
	$(Fe_{0.802}Ni_{0.198})_{0.927}S$	6.05	3.863	–3.759
	$(Fe_{0.601}Ni_{0.399})_{0.934}S$	7.27	5.236	–5.095
	$(Fe_{0.406}Ni_{0.594})_{0.934}S$	7.16	5.275	–5.132
	$(Fe_{0.202}Ni_{0.798})_{0.938}S$	5.68	3.950	–3.843
	$Ni_{0.953}S$	1.58	0	0
(b)	$(Fe_{0.401}Ni_{0.599})_{0.899}S$	7.75	0	0
	$(Fe_{0.403}Ni_{0.597})_{0.918}S$	7.50	0.015	–0.014
	$(Fe_{0.406}Ni_{0.594})_{0.934}S$	7.27	0	0
(c)	$Ni_{0.924}S$	2.24	0	0
	$Ni_{0.953}S$	1.58	0.085	–0.083
	$Ni_{0.982}S$	0.75	0	0

Table VI. Enthalpies of formation of $(Fe_{1-x}Ni_x)_{1-z}S$ solid solutions obtained from calorimetric measurements, $\Delta H_{f\text{-}exp}$, and calculated using Equation (6), $\Delta H_{f\text{-}cal}$.

Composition $(Fe_{1-x}Ni_x)_{1-z}S$	**$\Delta H_{f\text{-}exp}$ (kJ/mol)**	**$\Delta H_{f\text{-}calc}$ (kJ/mol)[†]**	**Composition $(Fe_{1-x}Ni_x)_{1-z}S$**	**$\Delta H_{f\text{-}exp}$ (kJ/mol)**	**$\Delta H_{f\text{-}calc}$ (kJ/mol)[†]**
$Fe_{0.875}S$	–94.4 ± 3.0[*]	–94.4	$(Fe_{0.601}Ni_{0.399})_{0.934}S$	–91.0 ± 2.9	–92.6
$Fe_{0.90}S$	–95.9 ± 4.0[*]	–95.8	$(Fe_{0.401}Ni_{0.599})_{0.899}S$	–89.3 ± 3.8	–88.2
$Fe_{11/12}S$	–97.3 ± 3.7[*]	–96.7	$(Fe_{0.403}Ni_{0.597})_{0.918}S$	–89.7 ± 3.2	–89.3
$Fe_{0.919}S$	–96.1 ± 2.8	–96.8	$(Fe_{0.406}Ni_{0.594})_{0.934}S$	–90.5 ± 3.0	–90.2
$Fe_{0.94}S$	–98.6 ± 3.0[*]	–98.0	$(Fe_{0.202}Ni_{0.798})_{0.938}S$	–86.0 ± 3.5	–87.8
$Fe_{0.96}S$	–99.2 ± 3.2[*]	–99.1	$Ni_{0.924}S$	–85.3 ± 4.1	–84.5
$Fe_{0.98}S$	–100.7 ± 4.2[*]	–100.2	$Ni_{0.953}S$	–86.0 ± 3.6	–86.1
FeS	–101.4 ± 4.0[*]	–101.3	$Ni_{0.982}S$	–88.2 ± 4.0	–87.7
$(Fe_{0.802}Ni_{0.198})_{0.927}S$	–94.1 ± 3.1	-94.8			

[*]Experimental data taken from Xu and Navrotsky (2010).
[†]Uncertainties of the calculated enthalpies are ± 1.8 kJ/mol according to the least squares regression analysis.

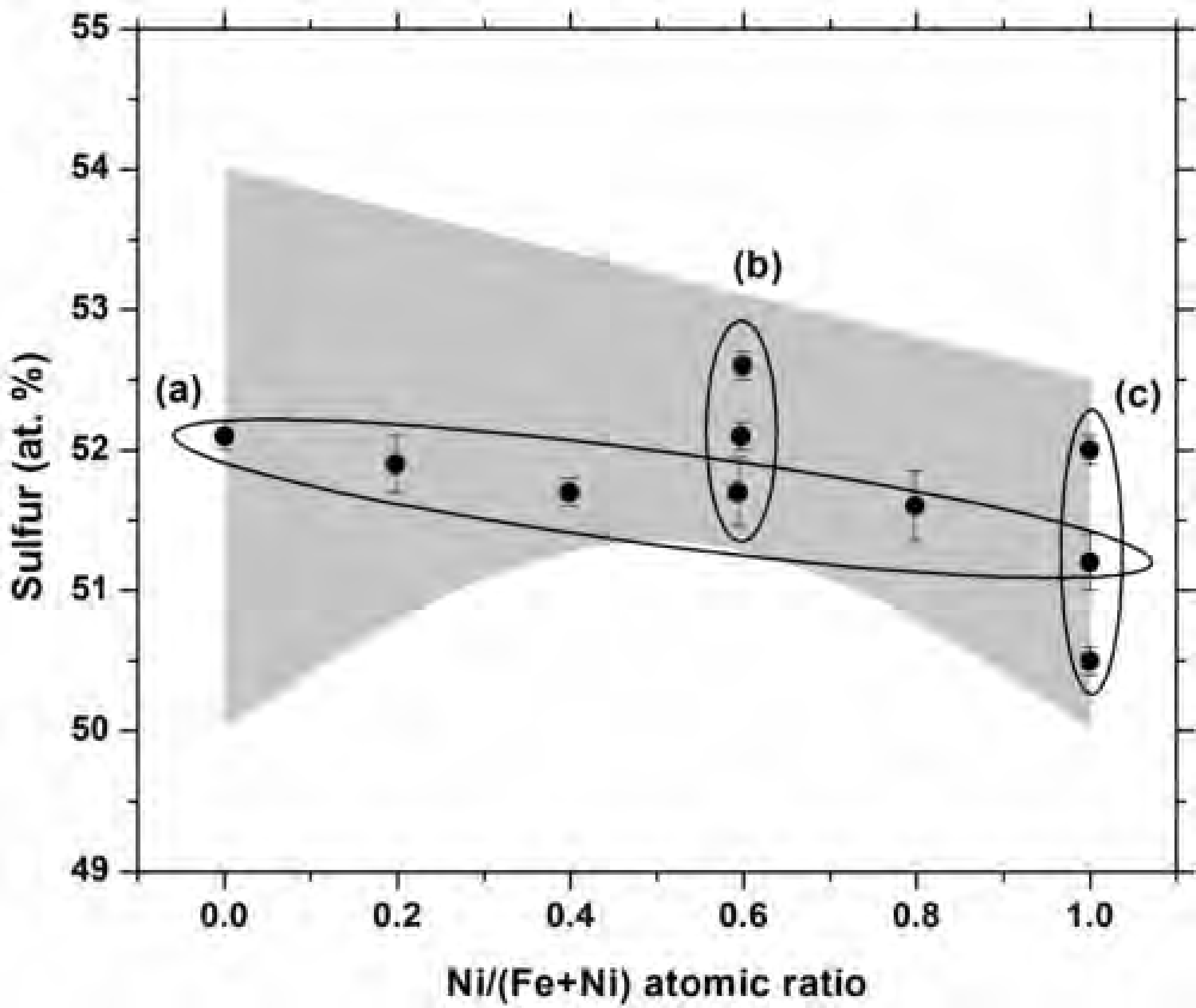
55
54
53
52
51
50
49
Sulfur (at. %)
(a)
(b)
(c)
0.0
0.2
0.4
0.6
0.8
1.0
Ni/(Fe+Ni) atomic ratio

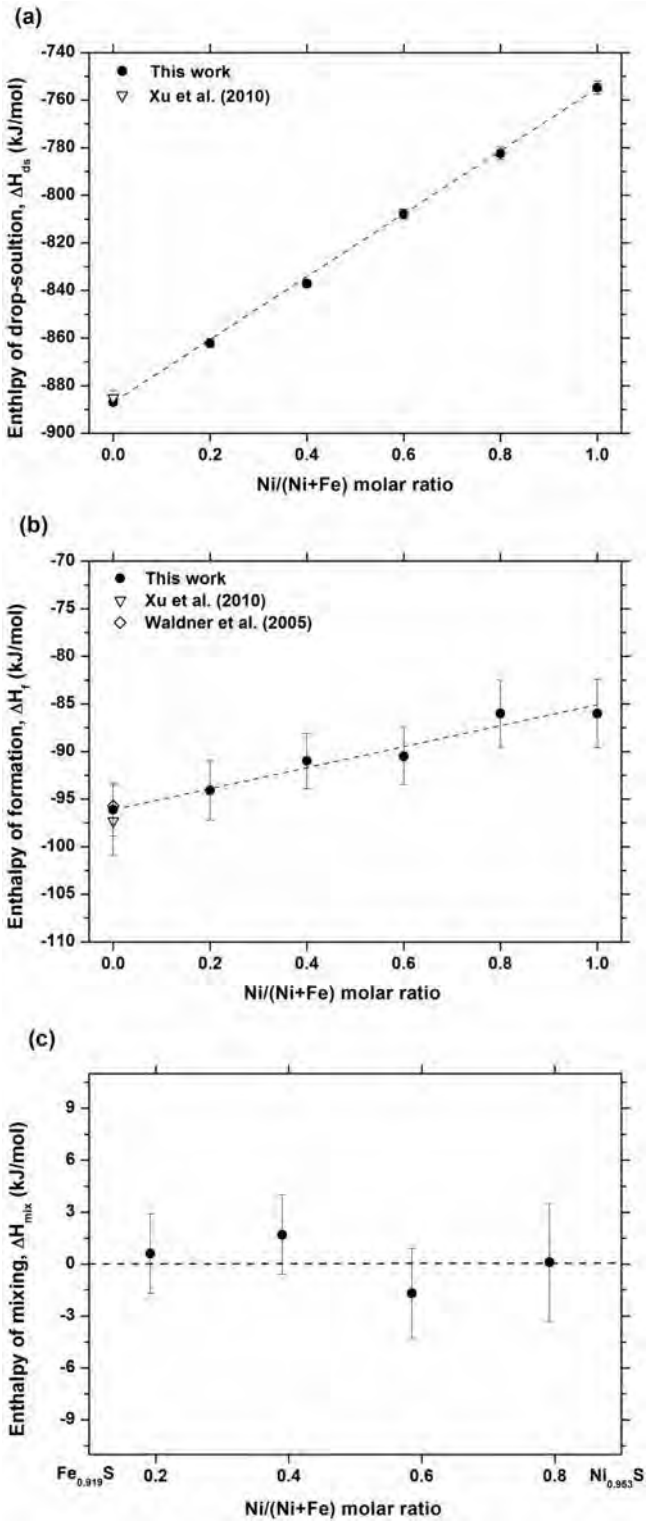
(a)
This work
Xu et al. (2010)
Enthlpy of drop-soultion, ΔH_{ds} (kJ/mol)
-740
-760
-780
-800
-820
-840
-860
-880
-900
0.0
0.2
0.4
0.6
0.8
1.0
Ni/(Ni+Fe) molar ratio
(b)
This work
Xu et al. (2010)
Waldner et al. (2005)
Enthalpy of formation, ΔH_f (kJ/mol)
-70
-75
-80
-85
-90
-95
-100
-105
-110
0.0
0.2
0.4
0.6
0.8
1.0
Ni/(Ni+Fe) molar ratio
(c)
Enthalpy of mixing, ΔH_{mix} (kJ/mol)
9
6
3
0
-3
-6
-9
$Fe_{0.919}S$
0.2
0.4
0.6
0.8
$Ni_{0.963}S$
Ni/(Ni+Fe) molar ratio

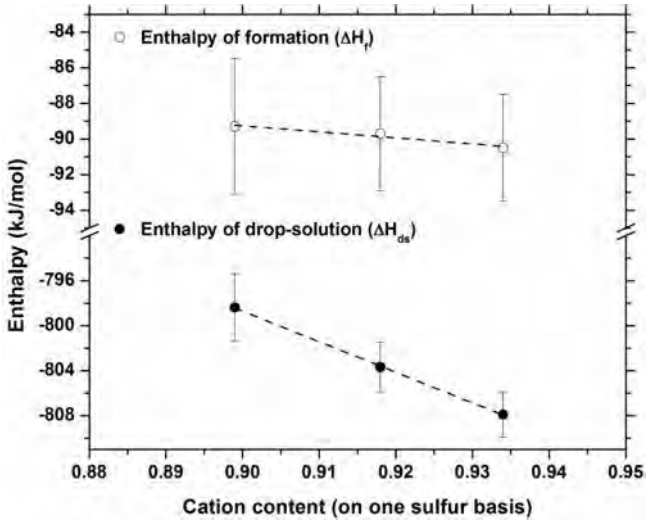
Enthalpy of formation (ΔH_f)
Enthalpy of drop-solution (ΔH_{ds})
Enthalpy (kJ/mol)
-84
-86
-88
-90
-92
-94
-796
-800
-804
-808
0.88
0.89
0.90
0.91
0.92
0.93
0.94
0.95
Cation content (on one sulfur basis)

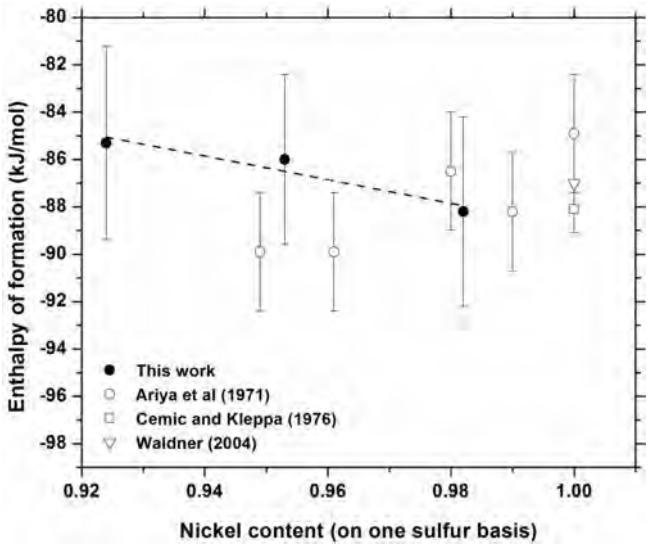
-80
-82
-84
-86
-88
-90
-92
-94
-96
-98
Enthalpy of formation (kJ/mol)
0.92
0.94
0.96
0.98
1.00
Nickel content (on one sulfur basis)
This work
Ariya et al (1971)
Cemic and Kleppa (1976)
Waldner (2004)

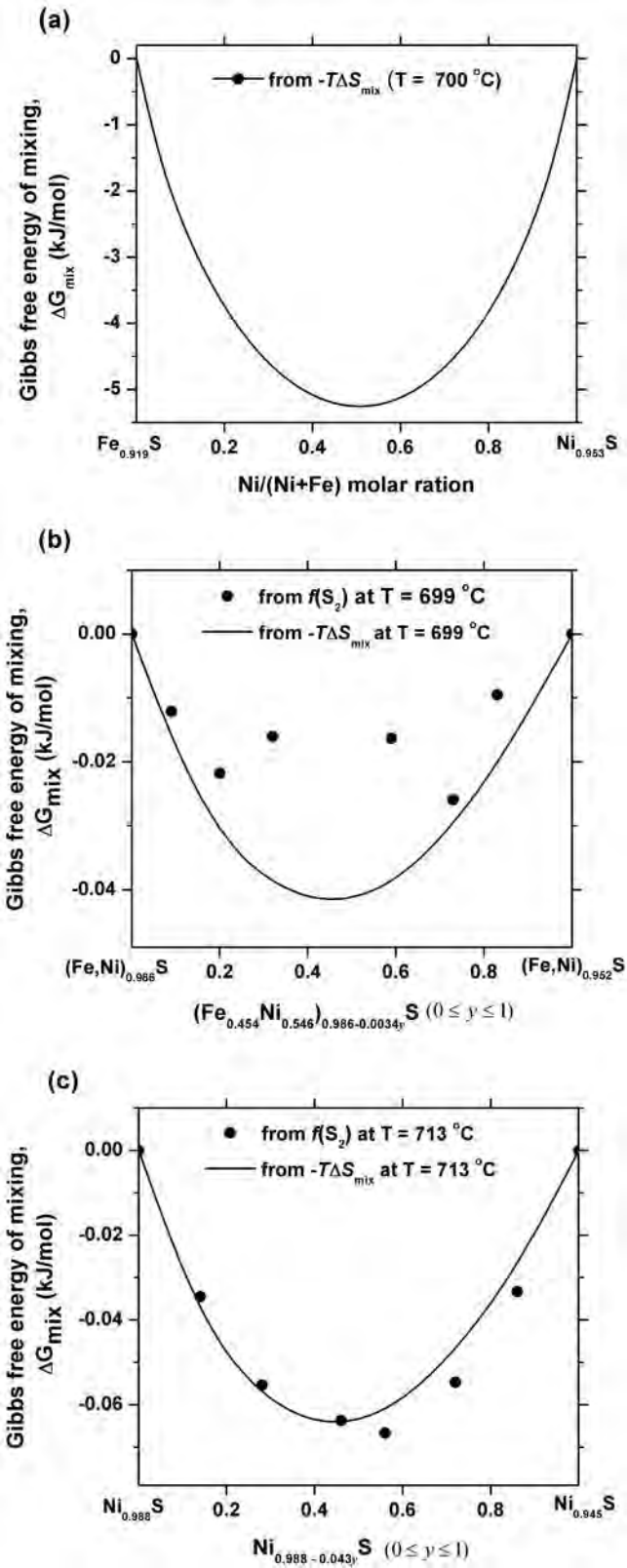
(a)
from -TΔS_mix (T = 700 °C)
Gibbs free energy of mixing, ΔG_mix (kJ/mol)
0
-1
-2
-3
-4
-5
Fe_0.919S
0.2
0.4
0.6
0.8
Ni_0.953S
Ni/(Ni+Fe) molar ration
(b)
from f(S_2) at T = 699 °C
from -TΔS_mix at T = 699 °C
Gibbs free energy of mixing, ΔGmix (kJ/mol)
0.00
-0.02
-0.04
(Fe,Ni)_0.966S
0.2
0.4
0.6
0.8
(Fe,Ni)_0.952S
(Fe_0.454Ni_0.546)_0.986-0.0034y S (0 ≤ y ≤ 1)
(c)
from f(S_2) at T = 713 °C
from -TΔS_mix at T = 713 °C
Gibbs free energy of mixing, ΔGmix (kJ/mol)
0.00
-0.02
-0.04
-0.06
Ni_0.988S
0.2
0.4
0.6
0.8
Ni_0.945S
Ni_0.988 - 0.043y S (0 ≤ y ≤ 1)